

Answer to Reviewer # 2

The authors thank the reviewer for his helpful comments on the paper. The necessary changes to the manuscript have been done according to the suggestions proposed. The remainder is devoted to the specific response of the reviewers' comments:

1. The reviewer is right. Not only plate ice crystals could explain high level of CALIOP backscattering in cirrus clouds. Such a feature could also be due to pristine-crystals like elongated columns, needles (and thin plates) which are preferentially oriented with their greater projected areas facing the fall direction. The abstract has been modified accordingly.

2, 3 and 4. Citations below have been added in the revised version of the manuscript.

Takano Y., and K.N. Liou: Solar radiative transfer in cirrus clouds. Part I: single-scattering and optical properties of hexagonal ice crystals. *J. Atmos. Sci.*, 45, 3–19, 1989.

Macke, A., J. Mueller, and E. Raschke: Single scattering properties of atmospheric ice crystals. *J. Atmos. Sci.*, 53, 2813–2825, 1996.

Iaquinta, J., H. Isaka, and P. Personne: Scattering phase function of bullet rosette ice crystals, *J. Atmos. Sci.*, 52, 1401–1413, 1995.

Field, P. R., A. J., Baran, P. H. Kaye, E. Hirst, and R. Greenaway: A test of cirrus ice crystal scattering phase functions, *Geophys. Res. Lett.*, 30, doi:10.1029/2003GL017482, 2003.

Baumgardner, D., H. Chepfer, G. B. Raga, and G. L. Kok: The shapes of very small cirrus particles derived from in situ measurements, *Geophys. Res. Lett.*, 32, L01806, doi:10.1029/2004GL021300, 2005.

Field, P. R., R. Wood, P.R.A. Brown, P.H. Kaye, E. Hirst, R. Greenaway, and J.A. Smith, J.: Ice particle interarrival times measured with a fast FSSP, *J. Atmos. Oceanic Technol.*, 20, 249–261, 2003.

5. Definition of the effective diameter.

According to Gayet et al. (2004) the effective diameter (D_{eff}) can be derived with the following relationship:

$$D_{eff} = A \times IWC / Ext$$

with D_{eff} expressed in μm , IWC (Ice water content) in g/m^3 , Ext (extinction coefficient) in km^{-1} and $A = 3000 \text{ mm}^3/\text{g}$. Both IWC and Ext relate contributions of ice particles measured from $3 \mu\text{m}$ (from FSSP-300 and CPI instruments).

6.1 Contribution to the volume extinction coefficient made by each of the classified habits.

Unfortunately, the PDF contributions to the extinction made by each of the classified habits cannot be provided due to a low number of particles in each of the categories. In other words, the number of particles in each of the classified habits is not sufficient to obtain good statistical significance of the PDF.

6.2 Although plates are common in both cases but do they also contribute most significantly to the measured volume extinction coefficient ?

We would like to underscore that the pie-chart representation (c) is done in Figs. 2 and 4 in terms of particle surface. This roughly gives the idea of the plates' contribution into the volume extinction coefficient. Very similar results are obtained for both cases by considering particle volume classification.

7. See revised version of the manuscript.

8. Unfortunately the humidity measurements are not reliable during the case A flight sequence.

9. Discussion on airmass origins.

Figures A.1 display two images from MSG satellite (Meteosat Second Generation) in the IR channel at 13:00 UT (case A) and 8:30 UT (case B). The corresponding flight areas where the observations have been carried out are superimposed by yellow ellipses on the figures. The satellite images clearly show that a cirrus band associated with a warm front was moving over France during the two Falcon flight periods. During the cirrus case A study the observations address the rear (and possibly dissipating) parts of the cirrus band while frontal (and likely dynamically active) part of the cirrus band was experienced during the case B sequence.

The back trajectory analysis may give some insight about the origin of the air mass in both clouds cases. The NOAA Hybrid Single-Particle Lagrangian Integrated Trajectory model (HYSPLIT, provided by the Air Resources Laboratory, Draxler and Rolph, 2003) was used to compute 5 days backward trajectories ending at 13:00 UT / 12000 m and 9:00 UT / 7100 m for cases A and B respectively. The results are displayed in A.2. The analysis reveals that the air mass travelled over 5 days mainly over the North Atlantic Ocean from Middle West of USA. These results indicate no significant differences between the origins of the air masses in the two experienced cirrus sectors. Despite the inherent limitations in the reliability of the results (because of different considered sources, i.e. 11000 m and 7500 m respectively, the clouds in the two sectors may process the aerosol differently before it reaches the points of measurement) the analyzed backward trajectories, at least, provide some basis for speculation about similar IN and therefore may not explain the observed differences in crystal internal structure properties.

10.1 Discussion section about the fraction of air within the modelled crystals as well as the assumed degree of roughness or distortions

The manuscript has been modified as the following :

... The smoothed scattering pattern (Fig. 2b) was obtained for the rough surface of crystals with a heavy load of inclusions. To be specific, the distortion parameter was of 0.1, which corresponds to a deeply rough surface according to the classification of Yang and Liou (1998); the mean free path length between two subsequent inclusions (see details in Macke et al., 1996) was equal to $0.15 \cdot D$, where D is the diameter of the circle circumscribing the hexagonal facet of an ice crystal. The scattering pattern with 22° halo (Fig. 4.b) was computed for the slightly rough surface of crystals that have no inclusions (the distortion parameter was of 0.01).

10.2 Error on the estimated asymmetry parameter from PN measurements

The asymmetry parameter is calculated with the relationships below (see Gerber, 2000) and applied to Polar Nephelometer data (Gayet et al., 2002) :

$$g = (f \cdot R3 + (R1 - R2) \cdot (1 - f)) / R3 \quad \text{with} \quad R1 = \int_{\theta_1}^{\pi/2} \cos \theta \cdot \sin \theta \cdot \psi(\theta) \cdot d\theta \quad (2)$$

$$R2 = \int_{\pi/2}^{\theta_2} |\cos \theta \cdot \sin \theta| \cdot \psi(\theta) \cdot d\theta \quad \text{and} \quad R3 = \int_{\theta_1}^{\theta_2} \sin \theta \cdot \psi(\theta) \cdot d\theta \quad (3)$$

Here $\psi(\theta)$ is the volume scattering coefficient measured at the scattering angle θ . Eq. (2) assumes that the diffraction and refraction components of the scattered light at small scattering angles $\theta_1 < 15^\circ$ and $\theta_2 > 162^\circ$ can be separated (Gerber et al., 2000). The ratio f of the diffracted portion of the scattered light to the total scattered light has been determined for non-absorbing large spheres to be $f = 0.56$ by using Mie calculations and by assuming typical measured water droplet spectra. Without any a priori information of water phase of cloud particles, the value of f is assumed also for ice particles. In fact, this value is close to the average value which can be estimated from the results of Garrett et al. (2001) obtained for a variety of ice crystal shapes. Nevertheless, due to deficiencies in theoretical approaches particularly for irregular shaped ice crystals significant uncertainties may remain in the g -value determination, but the relative fluctuations of this parameter probably reflect the actual cloud optical properties. The absolute error on the asymmetry parameter is expected to range approximately between ± 0.04 (Jourdan et al, 2010) and ± 0.05 for clouds dominated by large ice crystals.

Gerber, H., Y. Takano, T.J. Garrett, and P.V. Hobbs, Nephelometer measurements of the asymmetry parameter, volume extinction coefficient and backscatter ratio in Arctic clouds, *J. Atmos. Sci.*, 57, 3021-3034, 2000.

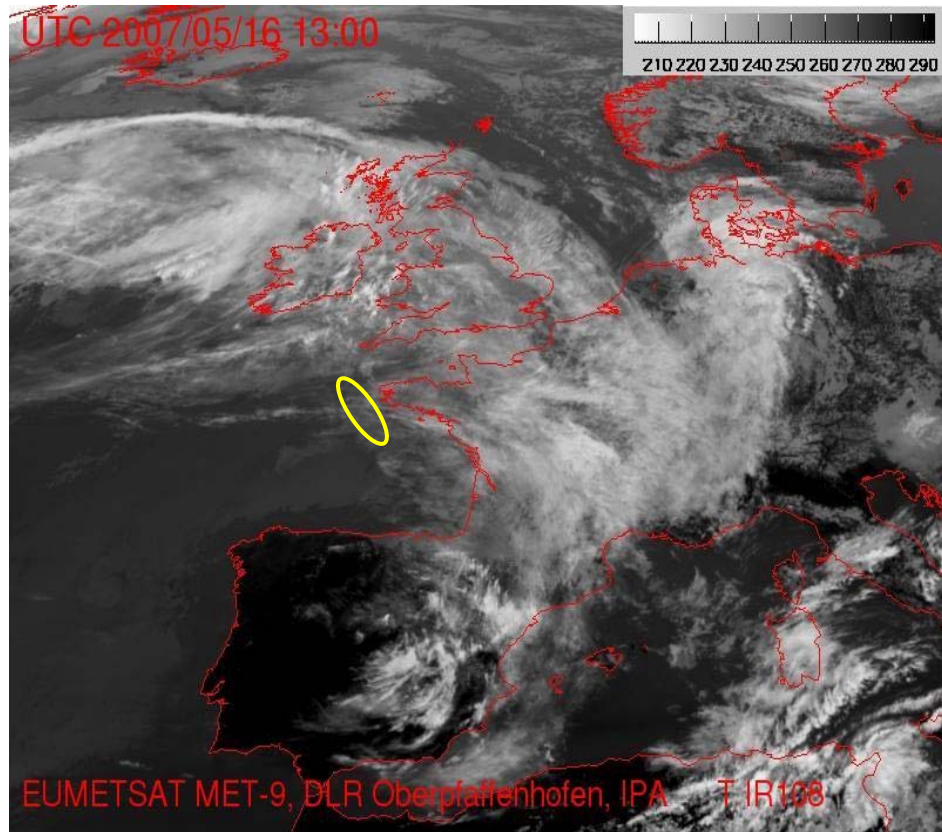
Gayet, J.F., S. Asano, A. Yamazaki, A. Uchiyama, A. Sinyuk, O. Jourdan and F. Auriol, Two case studies of winter continental –type water and mixed-phase stractocumuli over the sea, Part I : Microphysical and optical properties, *J. Geophys. Res.*, 107, D21, doi:10.1029/2001JD001106, 2002.

Garrett, T. J., P. V. Hobbs, and H. Gerber (2001), Shortwave, singlescattering properties of arctic ice clouds, *J. Geophys. Res.*, 106, doi:10.1029/2000JD900195, 2001.

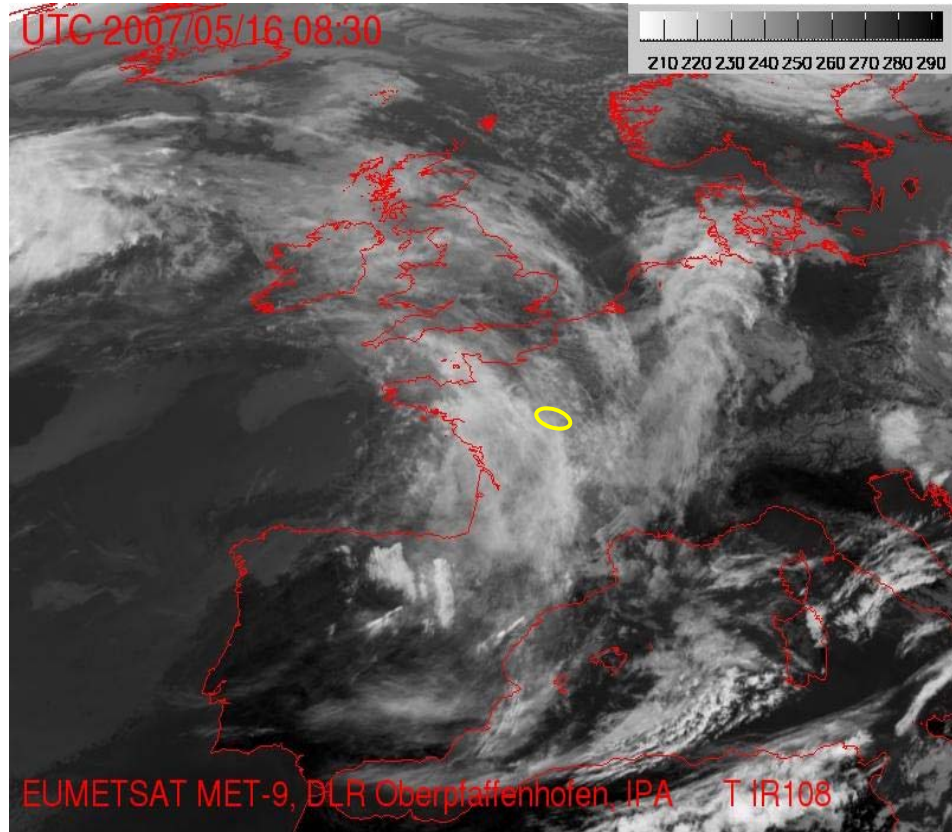
Jourdan O., G. Mioche, T.J. Garret, A. Schwarzenbock, J. Vidot, Y. Xie, V. Shcherbakov, C. Duroure, P. Yang and J-F Gayet: Coupling of the microphysical and optical properties of arctic clouds during the ASTAR 2004 experiment: Implications for light scattering modelling. *J. Geophys. Res.*, 115, doi:10.1029/2010JD014016, 2010.

11. The Baran (2009)'s reference is included in the revised version of the manuscript.

12. **Figures** : See revised version.

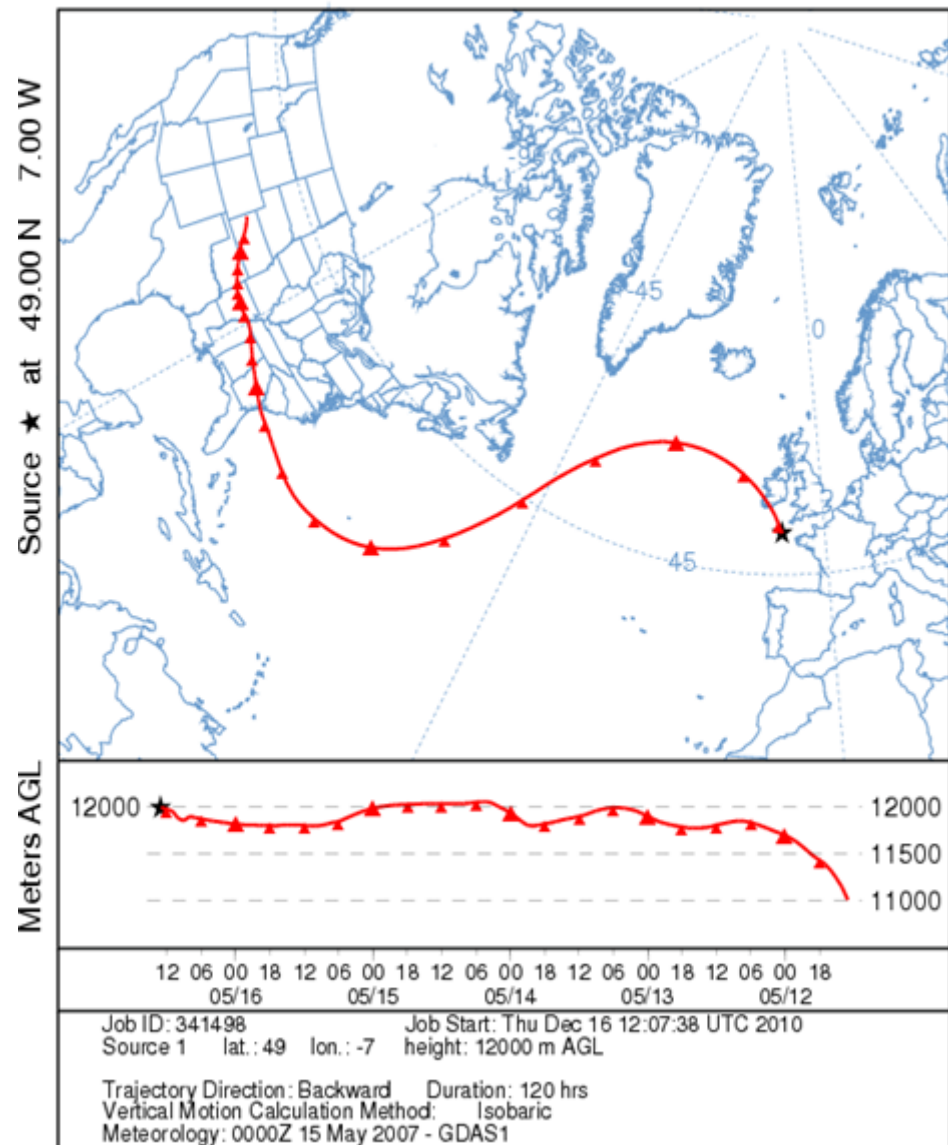


Cirrus case A (16 May 13:00 UT)



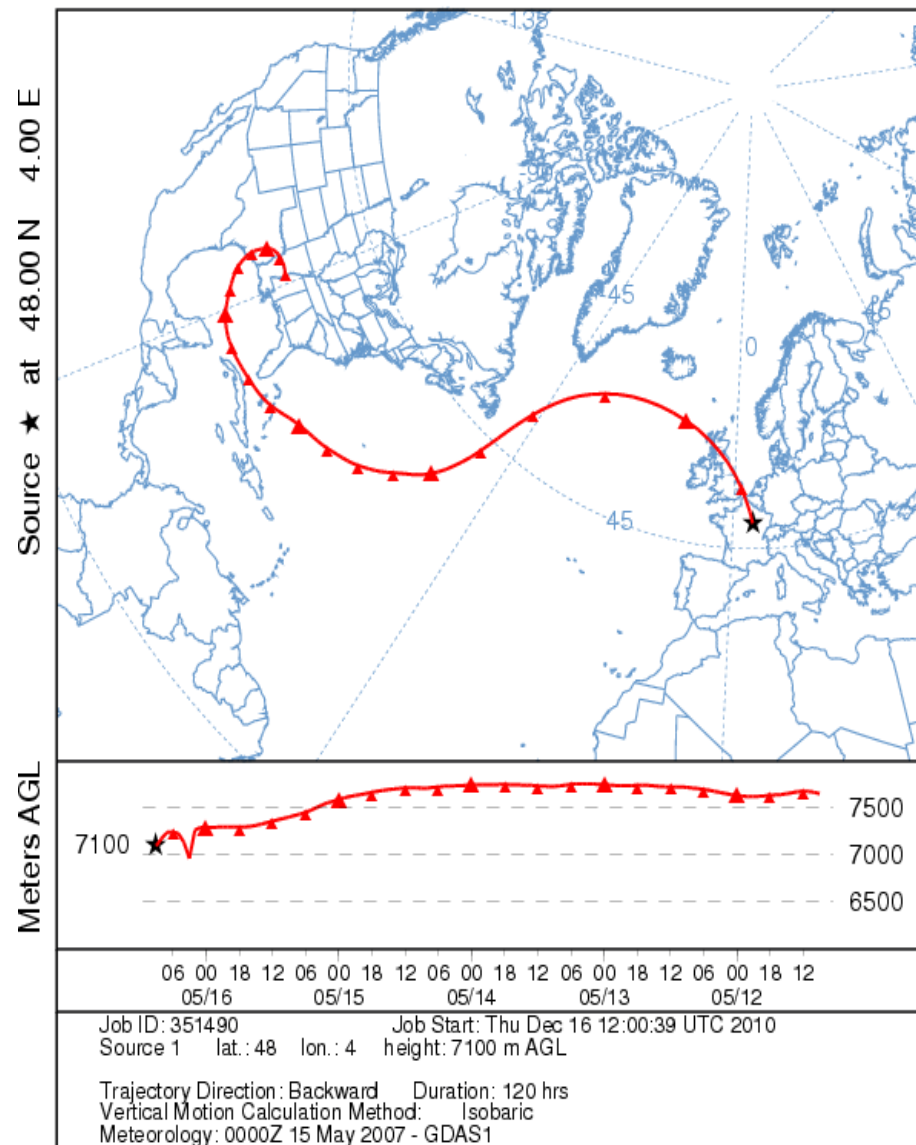
Cirrus case B (16 May 08:30 UT)

NOAA HYSPLIT MODEL
 Backward trajectory ending at 1300 UTC 16 May 07
 GDAS Meteorological Data



Cirrus case A (16 May 13:00 UT)

NOAA HYSPLIT MODEL
 Backward trajectory ending at 0900 UTC 16 May 07
 GDAS Meteorological Data



Cirrus case B (16 May 09:00 UT)